



1 **Fire-precipitation interactions amplify the quasi-biennial**
2 **variability of fires over southern Mexico and Central America**

3 Yawen Liu ^{1,2}, Yun Qian ^{3*}, Philip J. Rasch ^{3*}, Kai Zhang ³, Yuhang Wang ⁴, Minghuai Wang ^{1,2},
4 Hailong Wang ³, and Xiu-Qun Yang ¹

5 ¹School of Atmospheric Sciences, Nanjing University, China

6 ²Joint International Research Laboratory of Atmospheric and Earth System Sciences & Institute
7 for Climate and Global Change Research, Nanjing University, China

8 ³Pacific Northwest National Laboratory, Richland, Washington, USA

9 ⁴School of Earth and Atmospheric Sciences, Georgia Institute of Technology, Atlanta, Georgia,
10 USA

11 *Correspondence to:* Yun Qian and Philip J Rasch and (yun.qian@pnnl.gov and
12 Philip.Rasch@pnnl.gov)



13 **Abstract.** Fires have great ecological, social, and economic impacts. However, fire prediction and
14 management remain a challenge due to a limited understanding of their role in the Earth system.
15 Fires over southern Mexico and Central America (SMCA) are a good example, which greatly
16 impact local air quality and regional climate. Here we report that the spring-peak (Apr-May) fire
17 activities in this region have a distinct quasi-biennial signal based on multiple satellite datasets
18 measuring different fire characteristics. The variability is initially driven by the quasi-biennial
19 variations of precipitation. Composite analysis indicates that strong fire years correspond to
20 suppressed ascending motions and weakened precipitation over the SMCA. The anomalous
21 precipitation over the SMCA is further found to be mostly related to the East Pacific-North Pacific
22 (EP-NP) pattern two months previous to the fire season. The positive phase of EP-NP leads to
23 enhanced precipitation over the eastern US yet suppressed precipitation over SMCA, similar to the
24 spatial pattern of precipitation difference between strong and weak fire years. Meanwhile, the
25 quasi-biennial signals in precipitation and fires appear to be amplified by their interactions through
26 a positive feedback loop on short timescales. Model simulations show that in strong fire years,
27 more aerosol particles are released and transported downstream over the Gulf of Mexico and the
28 eastern US, where suspended light-absorbing aerosols warm the atmosphere and cause ascending
29 motions of the air aloft. Subsequently, a compensating downward motion is formed over the fire
30 source region and ultimately suppresses precipitation and intensifies fires. Statistical analysis
31 shows the different duration of the two-way interaction, where the fire suppression effect by
32 precipitation lasts for more than 20 days, while fire leads to a decrease in precipitation at shorter
33 time scales (3-5 days). This study demonstrates the importance of fire-climate interactions in
34 shaping the fire activities on interannual scale and highlights how precipitation-fire interactions at
35 short timescales contribute to the interannual variability of both fire and precipitation.



36 **1 Introduction**

37 Natural and human-induced fires are key features of the Earth system (Bowman et al., 2009).
38 Uncontrolled large fires damage biodiversity, affect human health, and incur high economic costs
39 (Knorr et al., 2017; Aguilera et al., 2021; Bowman et al., 2017). Comprehensive knowledge of
40 fires' causes, variability, and climate effects is necessary to accommodate or manage fires
41 effectively, and to mitigate adverse societal impacts.

42 Changes in climate alter fire regimes (Power et al., 2008; Jolly et al., 2015), because the occurrence
43 and intensity of fires depend on meteorological factors such as precipitation, wind, and humidity
44 (Flannigan et al., 2009; Marlon et al., 2008; Abram et al., 2021; Fang et al., 2021). Fires alter
45 weather and climate as well: they are important sources of aerosol particles that modify Earth's
46 energy and water budget either by directly absorbing and scattering sunlight or affecting cloud
47 microphysical processes (Voulgarakis and Field, 2015; Jiang et al., 2020; Liu et al., 2018; Yue et
48 al., 2022; Lu et al., 2018). There are many modes of interaction. The modes are complex, operate
49 through a variety of mechanisms, and manifest on a large variety of time and space scales (Ding
50 et al., 2021; Zhang et al., 2022). For example, Huang et al. (2023) have demonstrated that synoptic-
51 scale fire-weather feedback plays a prime role in driving extreme fires in the Mediterranean and
52 monsoon climate regimes over the US West Coast and Southeastern Asia. On interannual scales,
53 fires in the maritime subcontinent have been shown to affect SSTs, land temperature as well as
54 atmospheric stability, and influence ENSO on 3-6 year timescales (Tosca et al., 2010). The
55 extreme 2019-2020 Australian fires have also been demonstrated to contribute to the 2020-2022
56 strong La Niña event by enhancing cloud albedo, cooling and drying out the air, and forming a
57 positive feedback between the northward migration of intertropical convergence zone and sea
58 surface temperature cooling in the Niño3.4 region (Fasullo et al., 2023). Moreover, on even longer
59 timescales, fires can affect the accumulation of carbon dioxide and methane by modifying global
60 features like the Hadley circulation that change precipitation and temperature patterns and
61 eventually affect forest ecosystems to produce feedback operating over decades and centuries
62 (Crutzen and Andreae, 1990; Page et al., 2002; Tosca et al., 2013). It is hence necessary to explore
63 fire characteristics with special considerations of their multi-scale variability and feedback.

64 From a global perspective, fires occur progressively more frequently towards the tropics (Mouillot
65 and Field, 2005). Tropical savanna and forest burning contribute approximately 80% of global



66 open fire emissions (Bond et al., 2013). However, tropical regions also feature a great diversity of
67 climate-weather systems that affect fire occurrence and seasonality. In the tropical Northern
68 Hemisphere, fires over tropical southern Mexico and Central America (SMCA) occur during the
69 Feb-May dry season and peak in April-May (Magi et al., 2012). These fire activities have a
70 substantial influence on local air quality and human health (e.g., over Mexico City [19-20° N, 98-
71 100°W] and the Yucatan region (Crouse et al., 2009; Yokelson et al., 2007; Yokelson et al.,
72 2009). Fire emissions over the SMCA region also affect the eastern US after long-range transport
73 (Kreidenweis et al., 2001; Lee et al., 2006; Rogers and Bowman, 2001). Understanding the
74 processes that shape fire variabilities over this region is hence important locally (for air quality
75 and fire management) and over broader regions.

76 Here, for the first time, we report a distinct quasi-biennial variability of fire activities over the
77 southern Mexico and Central America region (SMCA, 10-25°N, 80-100°W) during the peak
78 burning months (April – May) over 2003-2019 by validating different fire characteristic with the
79 use of multiple independent datasets. We further explored the dominant causes of this quasi-
80 biennial signal and provided concrete evidence for positive fire-precipitation feedback on short
81 timescales to amplify the quasi-biennial signal based on model simulations.

82 **2 Data and Methods**

83 **2.1 Observations**

84 Two sets of fire emission inventories were used to investigate the interannual variability of fire
85 activities. The Global Fire Emissions Database with small fires version 4.1 (GFED v4.1s) is a
86 bottom-up inventory that generates fire-consumed dry matter using fire-burned areas combined
87 with emission factors (Giglio et al., 2013; Randerson et al., 2012). GFED v4.1s provides monthly
88 mean fire-consumed dry matter in total and for individual fire types at 0.25-degree spatial
89 resolution. The Quick Fire Emissions Dataset (QFED) is a top-down emission inventory that
90 generates fire emissions by using empirical relationships between fire consumption and fire
91 radiative power (Koster et al., 2015). Daily emissions of fire-emitted species at 0.1 horizontal
92 resolution from QFED version 2.5 were examined. Since the interannual variations of different
93 species are consistent, only variation of fire-emitted black carbon (BC) is shown here. We also
94 examined the interannual variation of fire-induced changes in aerosol optical depth based on the
95 MERRA-2 reanalysis data (Gelaro et al., 2017) and Level 3 version 4.2 CALIPSO satellite dataset



96 (Winker et al., 2013). For the MERRA-2 data, monthly mean BC aerosol optical depth (AOD) was
97 used for a better comparison with the BC emission from QFED emission data. The CALIPSO
98 product divides aerosol into six sub-types, and the gridded monthly mean 532nm AOD for the
99 biomass burning aerosol type under all-sky conditions was analyzed. We used the NOAA Climate
100 Data Record of Advanced Very High Resolution Radiometer (AVHRR) version 5 leaf area index
101 (LAI) (Vermote, 2019), which is defined as the one-sided green leaf area per unit ground surface
102 as a proxy for fuel load. Daily LAI product is provided on a 0.05-degree grid. The average of LAI
103 in the 10 days previous to the burning season is examined.

104 In order to investigate the climate influence on fire activities, we analyzed monthly mean
105 temperature and maximum temperature from the Climatic Research Unit gridded Time Series
106 (CRU TS) version 4.06 (Harris et al., 2014). The dataset is constructed based on station
107 observations and provides monthly data over the global land surface at 0.5-degree resolution. Apart
108 from the CRU dataset, two sets of satellite observations of precipitation were analyzed: the
109 monthly Integrated Multi-satellitE Retrievals for GPM (IMERG) precipitation estimates at 0.1
110 degrees (Huffman et al., 2015) and the 1-degree daily (version 1.3), 2.5-degree monthly
111 (version 2.3) Global Precipitation Climatology Project (GPCP) precipitation estimates (Adler et al.,
112 2018; Adler, 2017). IMERG is intended to intercalibrate and merge satellite microwave
113 precipitation estimates together with microwave-calibrated infrared satellite estimates and
114 precipitation gauge analyses (Huffman et al., 2020). Monthly mean 500hPa vertical velocity (ω)
115 at 2.5 degrees from NCEP/NCAR reanalysis (Kanamitsu et al., 2002) and 10m wind speed at 0.25
116 degrees from ERA5 reanalysis (Hersbach et al., 2020) were also used in our work. In order to
117 understand the interannual variation of precipitation, we examined the relationship between
118 precipitation and ten different teleconnection patterns, including Atlantic Meridional Mode
119 (AMM), East Pacific/North Pacific Oscillation (EP/NP), ENSO, North Atlantic Oscillation
120 (NAO), North Tropical Atlantic index (NTA), Pacific North American index (PNA), Tropical
121 Northern Atlantic index (TNA), Tropical Southern Atlantic index (TSA), Western Hemisphere
122 warming pool (WHWP), Quasi-biennial Oscillation (QBO). These indices and their detailed
123 definitions can be obtained from <https://psl.noaa.gov/data/climateindices/list/>.



124 **2.2 Model experiment**

125 The CESM2.1.0 model with the Community Atmosphere Model version 6 (CAM6) (Danabasoglu
126 et al., 2020) was used to investigate the feedback of fire-emitted aerosols on precipitation. The
127 F2000 component set was used with the prescribed sea surface temperature in the year 2000. The
128 horizontal resolution is set as 0.9-degree latitude by 1.25-degree longitude with 32 vertical levels.
129 Two groups of simulations were conducted. Each was driven by the representative fire emissions
130 in strong and weak fire years and referred to as Case_Strong and Case_Weak. The difference in
131 variables (e.g., temperature and precipitation) between the two cases (Case_Strong minus
132 Case_Weak) indicate the influence, or difference in feedback, caused by stronger fire emissions.
133 As our work focused on the influence of fire activities over SMCA, only fire emissions over the
134 SMCA region were considered. The default fire emission inventory (Van Marle et al., 2017) in
135 CESM2.1.0 was modified accordingly while global anthropogenic emissions are kept unchanged
136 and remain the same between cases. Given that composite analysis indicates fire emissions in weak
137 fire years are approximately half those in strong fire years. We simply used the average of fire
138 emissions during strong fire years in Case_Strong, and reduced these by half in Case_Weak. More
139 subtle changes in fire locations between strong and weak fire years are hence ignored. Furthermore,
140 global climate models have long been found to underestimate fire-induced changes in aerosols
141 (Zhong et al., 2022). Hence, in order to ensure the simulated difference in fire-induced AOD
142 between Case_Strong and Case_Weak is comparable to observations, the default inventory is
143 multiplied by a factor of 3 to ensure the simulated fire-induced AOD changes are comparable to
144 observations. For each group, 9 ensemble simulations were performed with slight differences in
145 their initial conditions. The ensemble mean is calculated as the average of 9 members. All
146 simulations start on Jan.1 with a 3-month spin-up time. The T-test is used to identify statistically
147 significant differences between Case_Strong and Case_Weak.

148 **3 Results**

149 **3.1 Biennial variability of fire activities**

150 We focus on the southern Mexico and Central America region (SMCA) covering both the Yucatan
151 region and Mexico City. Major fire types in this region consist of deforestation fires, savanna fires,
152 and agricultural waste burning, which respectively are estimated to consume 45.5%, 42.1%, and



153 12.40% of the total burned dry matter during the peak burning months (Apr-May) of the 17-year
154 (2003-2019) study period.

155 As shown in Fig. 1a, GFEDv4.1s estimates of the regional sum of the total dry matter consumed
156 by fire activities feature obvious quasi-biennial variability. Generally speaking, fire activities in
157 odd-numbered years show higher consumption of dry matter than adjacent even-numbered years
158 with the only exception of the year 2016, which might be related to a long-lasting El Niño event
159 spanning 2014-2016. Composites of fire consumption indicate enhanced fire activities along both
160 sides of the high terrains in odd-numbered years, and the most profound difference appears over
161 the bordering area between southern Mexico and Guatemala (Fig. S1). The fire-consumed dry
162 matter here differs by more than a factor of 6 between odd-numbered and even-numbered years.

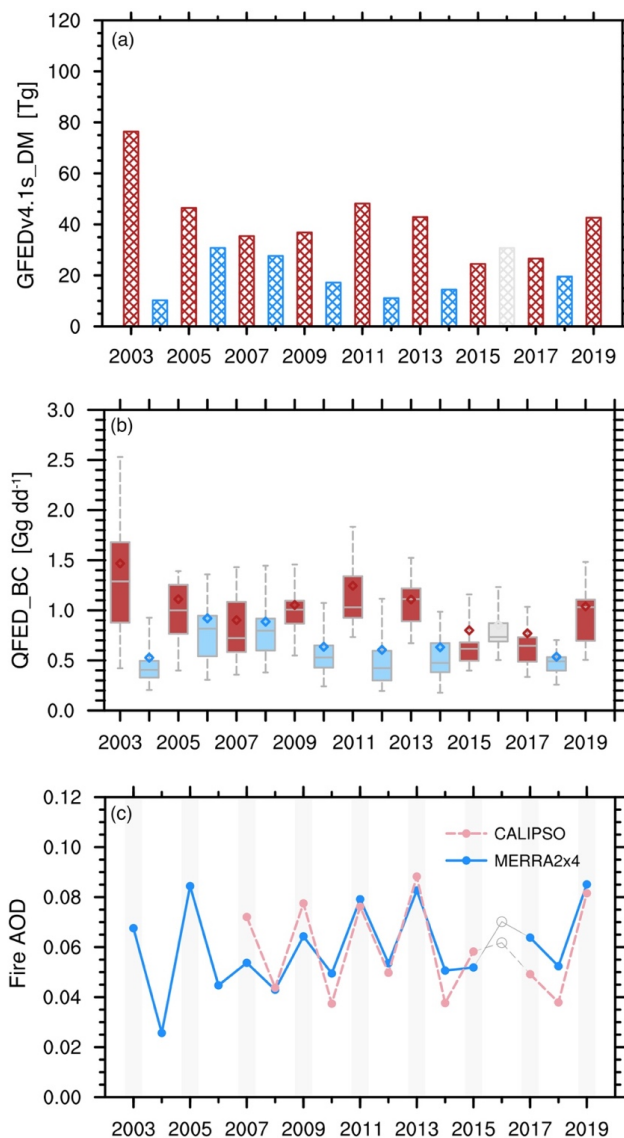
163 The quasi-biennial variability of fire activities is also evident when examining fire emissions of
164 typical fire-emitted species based on the QFED inventory (Fig. 1b). Similarly, fire-emitted BC in
165 odd-numbered years is basically higher than those in the adjacent even-numbered years, when
166 considering both regional mean and medium values. Furthermore, among the 9 odd-numbered
167 years, fire activities in years 2003/2011/2013 show the highest three BC emission, which is also
168 consistent with results from the GFEDv4.1s dataset. Hence, the two independent fire emission
169 inventories agree on the interannual variation of fire activities.

170 Apart from cross-checking different fire emission inventories, we further validated the variability
171 of fire activities by investigating fire-induced changes in AOD (Fig. 1c). BC AOD from MERRA-
172 2 reanalysis and AOD of biomass burning aerosol type from CALIPSO were adopted to represent
173 fire activities. Basically, the interannual variation of fire-related AOD in both datasets agrees well
174 with the estimates from fire inventories, thus providing additional support for the quasi-biennial
175 variability of fire activities in the peak burning months over SMCA. Overall, the intercomparison
176 between multiple datasets indicates a consistent quasi-biennial variability in different fire
177 characteristics, including fire-consumed dry matter, fire-emitted aerosols as well as fire-related
178 changes in optical properties. To describe this quasi-biennial variability for convenience, we
179 hereafter refer to the odd-numbered (even-numbered) years that have higher (lower) fire
180 consumptions than adjacent years as strong (weak) fire years.

181



182



183

184

185 **Figure 1.** Interannual variations of different fire characteristics during the peak burning season
 186 (Apr-May) over Southern Mexico and Central America (SMCA). (a) Regional sum of the total dry
 187 matter consumed by fire activities based on the GFEDv4.1s emission data. (b) Distributions of the
 188 daily sum of fire-emitted black carbon (BC) over SMCA based on QFED emission data. Boxes
 189 denote the 25th and 75th percentiles. Bars outside the boxes denote the 10th and 90th percentiles.
 190 Bars within the boxes denote the medium values, and dots denote regional mean values (c)
 191 Regional mean aerosol optical depth (AOD) of smoke aerosols from CALIPSO product and BC
 192 AOD from MERRA-2 reanalysis. The odd-numbered years with strong fires are denoted by the
 193 grey bars.
 194



195 **3.2 Dominant role of the biennial variability of precipitation**

196 Fire activity is strongly affected by factors including fire ignition, fuel load, and climate-weather
197 conditions (Flannigan et al., 2005; Archibald, 2016; Ichoku et al., 2016; Veira et al., 2016). Fire
198 ignition is affected by both natural lightning and human activities (Pechony and Shindell, 2009).
199 Since there has no policy to regulate fire activities with periodicity, it is unlikely that human impact
200 is the major driving force. Fuel availability may play a role in the interannual variation of fires,
201 but there is little evidence for it in the leaf area index, our surrogate for fuel load (Fig. S2).
202 Correlations between LAI previous to the burning season and fire consumption are statistically
203 insignificant.

204 Close yet complex relationships between ambient conditions (e.g., humidity, temperature,
205 precipitation) and fire activities have been widely revealed in previous studies (Cary et al., 2006;
206 Gillett et al., 2004; Prasad et al., 2008). For example, warm temperatures could increase fire
207 activity by increasing evapotranspiration and also by lengthening fire duration, while both the
208 timing and amount of precipitation could regulate fire behavior. To identify the climatic factors
209 that might be responsible for the quasi-biennial variation of fire activities, we first examined the
210 relationships between fire consumption and different meteorological variables (Table 1). Temporal
211 correlations of their regional mean values indicate that fire activities are enhanced with warmer
212 mean and maximum temperature ($R=0.47$ and 0.59), but are weakened with higher precipitation
213 ($R=-0.69$). Though wind speed could affect the spread of fire activities, the insignificant
214 correlation signifies a minor influence on the interannual scale.

215 Figure 2 shows the spatial distribution of correlations of fire consumption with precipitation and
216 mean temperature during peak burning months. With respect to precipitation, negative correlations
217 cover almost the entire SMCA region and are statistically significant over major fire source areas
218 from Yucatan extending southwestward to Chiapas. In contrast, positive correlations between fire
219 consumption and maximum temperature mainly appear over the northern part of SMCA (southern
220 Mexico), albeit with less influence over Central America (e.g., fire source areas in Guatemala).
221 Hence, the interannual variability of precipitation affects the variation of fire activities on a wider
222 spatial range. We next examined closely the time series of regional mean precipitation and
223 temperature (Fig 3). Here regional mean values are calculated using data over land so that only
224 climate conditions that could directly affect fire activities are considered. Two independent
225 precipitation datasets show similar temporal evolution patterns. An obvious quasi-biennial



226 variability is seen in regional mean precipitation. More suppressed precipitation (compared to
227 adjacent years) corresponds well to the strong fire years (excluding the year 2016). Furthermore,
228 spectral analysis confirms a statistically significant periodicity of approximately 2 years (0.042
229 cycles per month) for precipitation, suggesting the mediation of precipitation on the quasi-biennial
230 feature of fire activities. Meanwhile, the quasi-biennial signal is less apparent in mean and
231 maximum temperatures. For instance, temperatures in the strong fire years 2007 and 2009 are
232 smaller in magnitude compared to adjacent weak fire years. Nevertheless, higher mean and
233 maximum temperatures (compared to adjacent years) appear in 2003 and 2011, which combines
234 with the suppressed precipitation, contributing to the abnormally high fire consumption in the two
235 years. As a result, while both temperature and precipitation are critical in shaping fire activities
236 over the SMCA region, precipitation plays a more fundamental role in formulating the quasi-
237 biennial variability of fires.

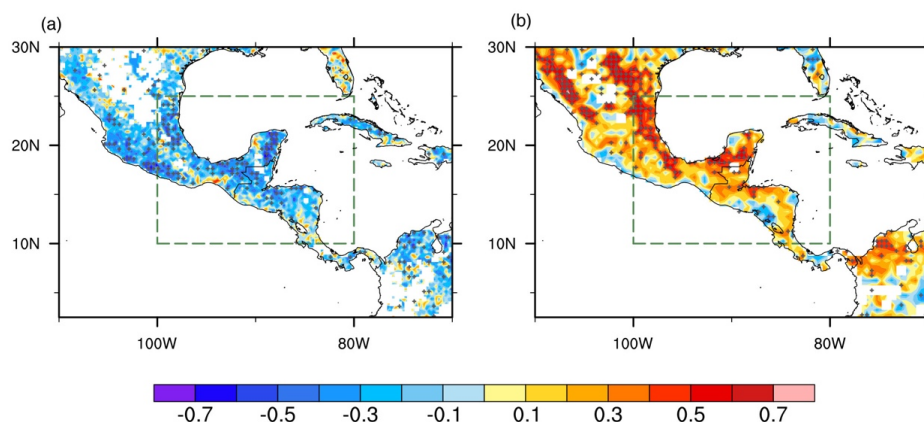
238

239 **Table 1.** Correlations between the regional sum of fire consumed dry matter based on the
240 GFEDv4.1 data and regional mean values of different meteorological variables (including the
241 monthly mean precipitation from IMERG dataset, mean temperature, maximum temperature from
242 CRU dataset, and 10m wind speed from ERA5 reanalysis) averaged in the peak fire season (April-
243 May).

Correlation	Precipitation	Mean Temperature	Maximum Temperature	10m wind speed
Fire-consumed Dry matter	-0.69*	0.47*	0.59*	0.29

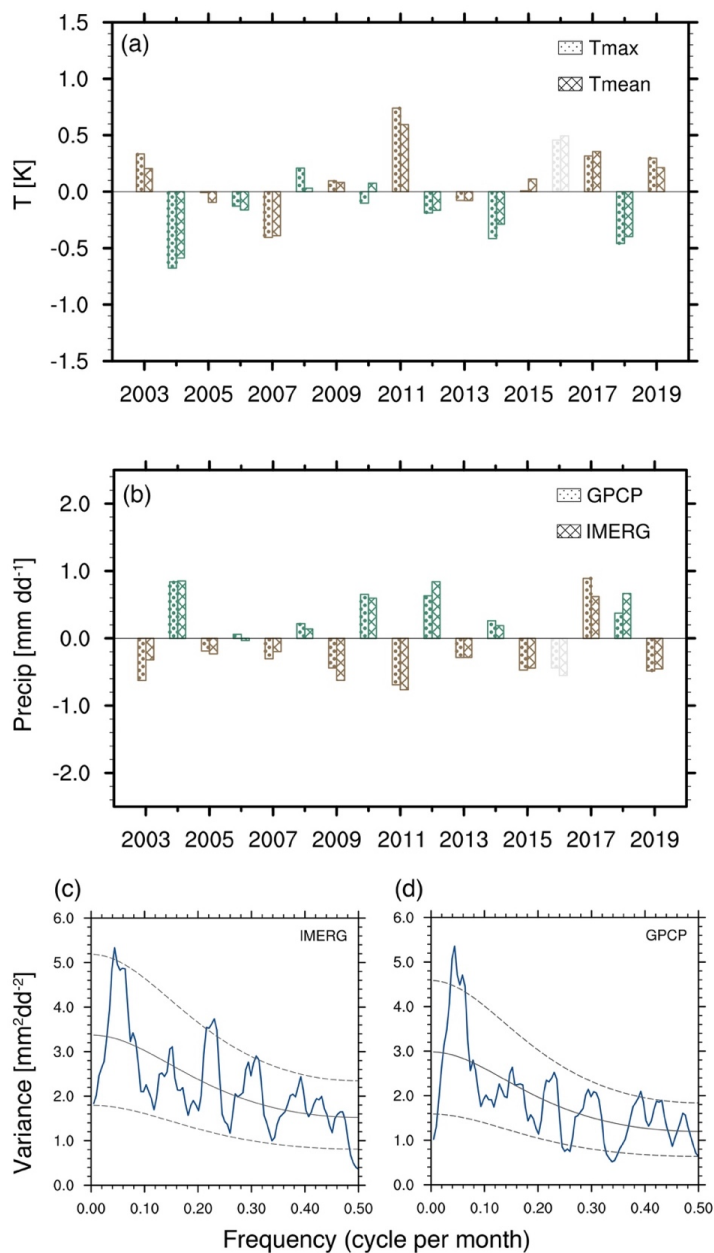
244 * represents the correlations are statistically significant at the 90% confidence level based on the
245 student's T-test.

246



247
248
249
250
251
252
253

Figure 2. The influence of meteorological factors on fire activities over SMCA. Spatial distributions of grid-to-grid correlations between fire-consumed dry matter and (a) precipitation from IMERG and (b) maximum temperature from CRU during the peak fire season (Apr-May) over 2003-2019. Stippling indicates the correlations are statistically significant at the 90% confidence level based on the student's T-test. The green boxes denote the SMCA region.



254
255
256
257
258
259
260
261

Figure 3. Interannual variability of meteorological factors in peak fire season over SMCA. Time series of the Apr-May (a) mean/maximum temperature and (b) mean precipitation anomalies averaged over SMCA (land only). (c) Spectral analysis of monthly mean precipitation averaged over SMCA during 2003-2019. The black solid line and dashed lines represent the red noise curve and the 10%, 90% confidence interval.

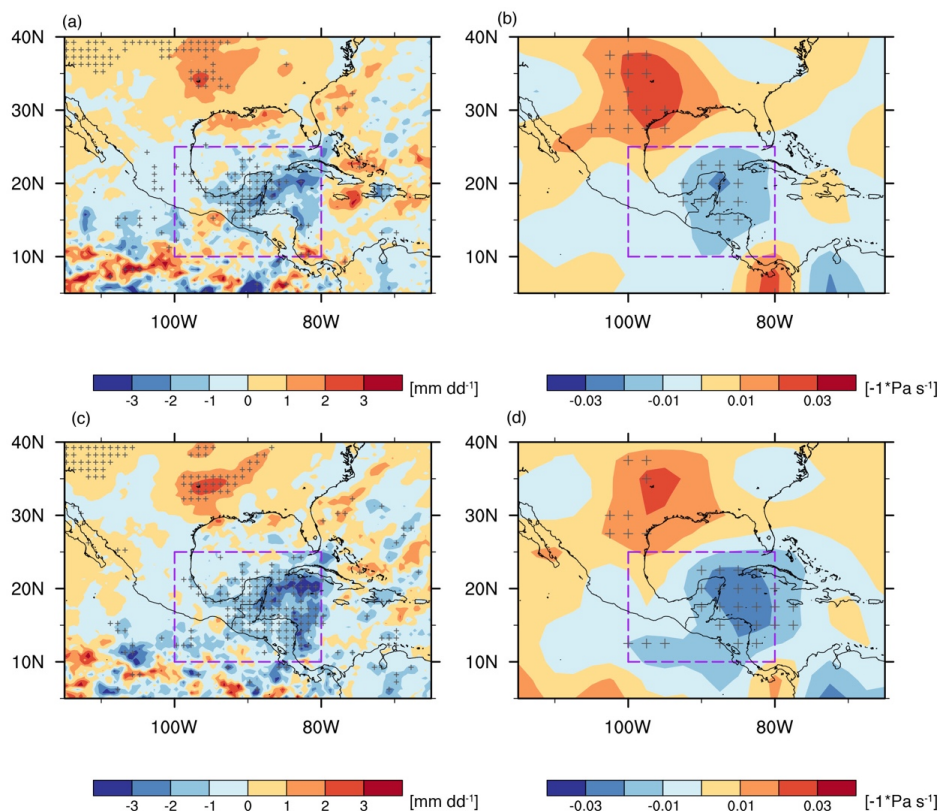


262 The leading role of precipitation on the interannually varying fire activities is evident in the
263 composite analysis, as shown by the contrast of reduced precipitation in strong fire years and
264 enhanced precipitation in weak fire years (Fig. 4a). The composite analysis further shows that the
265 anomalous precipitation is closely related to vertical motions, with stronger subsidence
266 corresponding to weaker precipitation (Fig. 4b). It is worth noting that to the northwest of the
267 SMCA region near the southeast US, composited precipitation and vertical velocity also differ
268 significantly between strong and weak fire years albeit of opposite signs. Consistent changing
269 features of precipitation and vertical velocity are also captured when regressing the two variables
270 on the regional mean precipitation over SMCA (Fig. 4c-d). The negative regression coefficients
271 indicate a stronger upward (downward) motion corresponding to higher (weaker) precipitation. In
272 sum, for a specific year, stronger subsidence and the subsequent suppression of precipitation tend
273 to amplify fire activity in that year, and vice versa for the year with weakened subsidence and less
274 suppression effect of precipitation. In this way, the quasi-biennial variability of precipitation leads
275 to the same interannual variability of fire activities.

276 Precipitation patterns over the SMCA region and the variability are associated with complex
277 physical forcing mechanisms, e.g. changes in sea surface temperature, low-level winds, the
278 strength and position of ITCZ et al., and all of these processes could be modulated by large-scale
279 modes of atmospheric and oceanic variability (Duran-Quesada et al., 2017; Perdigon-Morales et
280 al., 2019; Amador et al., 2006). Here we chose 10 typical teleconnection patterns, for example, the
281 El Niño-Southern Oscillation, (ENSO), based on previous studies and examined their relationships
282 with SMCA precipitation in the peak fire months. After calculating the correlations between Apr-
283 May mean precipitation and the index in varying months (both simultaneously and previous to the
284 fire season), we found that the precipitation in the fire season is mostly affected by the East
285 Pacific/North Pacific Oscillation (EP/NP) pattern in the previous two months (Feb-Mar).
286 Generally, the positive phase of EP/NP features negative height anomalies and an enhanced
287 cyclonic circulation over the eastern United States (Athanasiadis et al., 2010). Consequently, in
288 the following fire season, this causes anomalous upward and downward motions over the
289 southeastern US and the SMCA region respectively (Fig. S3), and enhances precipitation over the
290 southeastern US yet suppressing precipitation over the SMCA region (Fig. 5). Hence, the EP/NP
291 teleconnection results in an opposite responding pattern in precipitation and vertical velocity



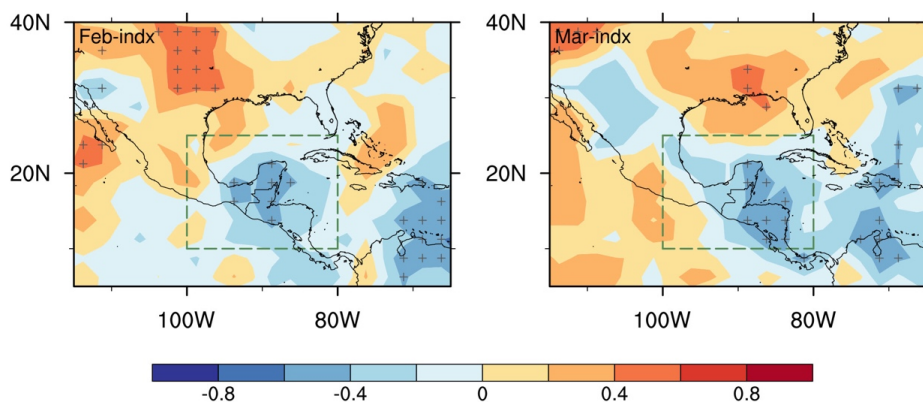
292 between the eastern US and the SMCA region. This further explains the similar contrasting spatial
293 pattern that is found in the aforementioned composite and regression analysis.



294
295

296 **Figure 4.** Varying characteristics of precipitation and circulations. Differences of composites of
297 (a) precipitation and (b) 500hPa vertical pressure velocity (reversed signs) between strong and
298 weak fire years. Stippling indicates the differences are statistically significant at the 90%
299 confidence level based on T-test. Regressions of Apr-May mean (c) precipitation and (d) 500hPa
300 vertical velocity on the regional mean precipitation over SMCA (reversed signs) during 2003-
301 2019. Stippling indicates regression coefficients are statistically significant at the 90% confidence
302 level based on the T-test.

303



304

305

306

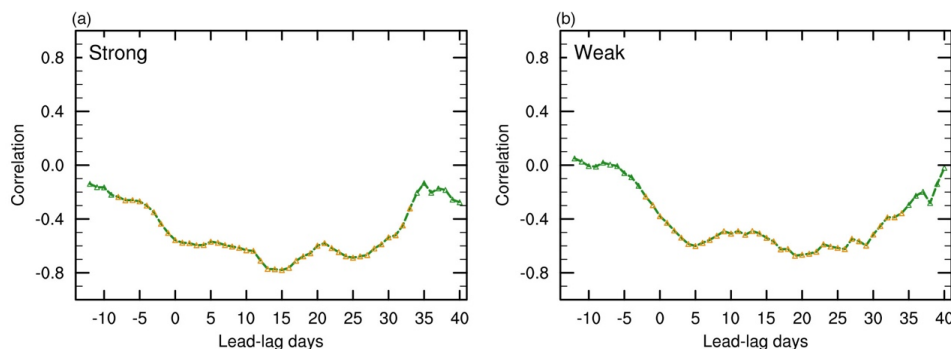
307

308

309

310

Figure 5. Influence of the EP/NP teleconnection pattern on precipitation in peak fire season. Spatial distributions of correlations of EP/NP index in (a) February and (b) March with the mean precipitation in the peak fire season (Apr-May) during 2003-2019. Stippling indicates the correlations are statistically significant based on the student's T-test.



311

312

313

314

315

316

317

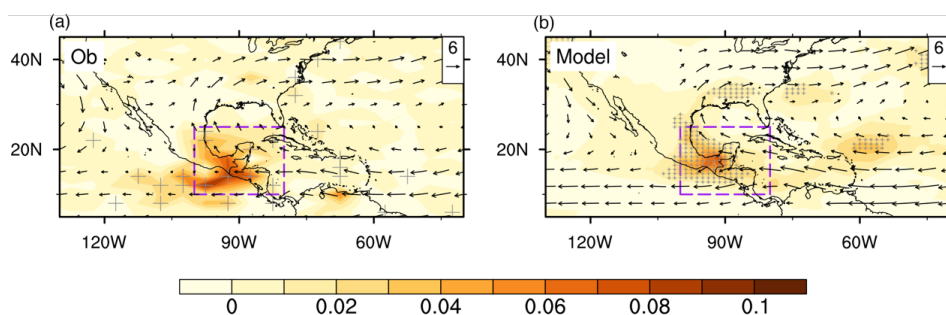
Figure 6. Different duration of fire-precipitation interaction. Lead-lag correlations between regional mean daily precipitation and fire emission composites in (a) strong fire years and (b) weak fire years over SMCA. Positive lead-lag days represent that precipitation leads while negative lead-lag days represent fire emissions leads. Correlations that are statistically significant at the 90% confidence level based on Student's t-test are marked with yellow triangles.



318 **3.3 Positive feedback between enhanced fire emissions and suppressed precipitation**

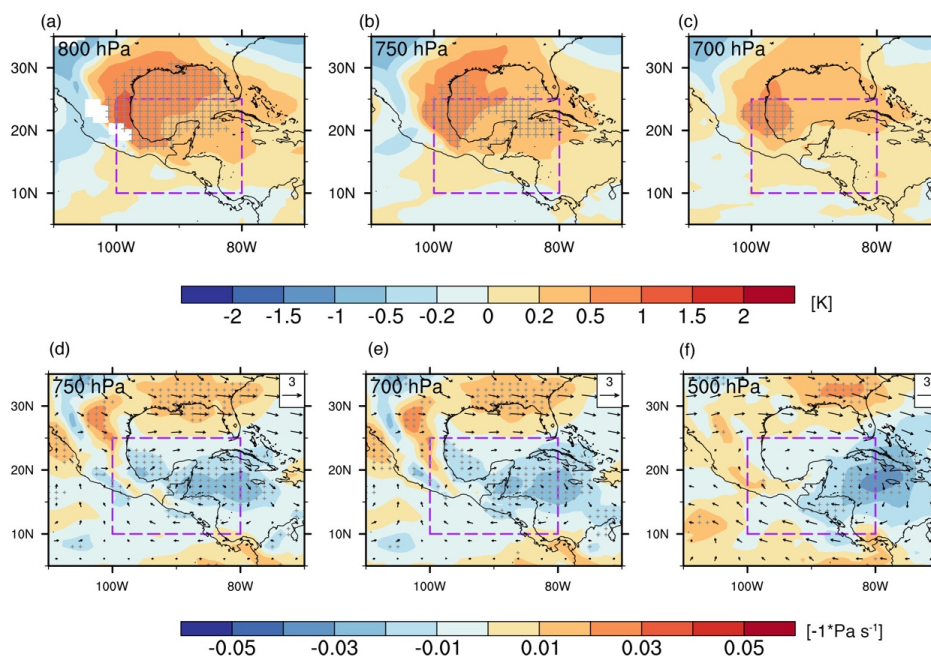
319 Previous studies have found that fire-emitted aerosols could interact with synoptic weather, which
320 in turn affects fire variability (Huang et al., 2023). In view of this, one concern is if fire and
321 precipitation interact on short timescales (i.e., within individual fire seasons) in our case over the
322 SMCA region, and if so, how this feedback modulates the quasi-biennial variability of
323 precipitation and fire activities. We first calculated lead-lag correlations between daily
324 precipitation and fire emissions to identify the short-term fire-precipitation interaction. As shown
325 in Fig. 6 lead-lag correlations between regional mean precipitation and fire emission are generally
326 similar whether fire activities in strong or weak fire years are considered. When precipitation leads,
327 precipitation negatively correlates with fire emission for more than 20 days, signifying a long-
328 lasting suppression effect of precipitation on fire activities. In other words, weakened precipitation
329 would enhance fire activities. Meanwhile, when fire leads, negative correlations indicate that
330 increased fire activities would further suppress precipitation at shorter timescales (3-5 days)
331 through rapid adjustments. In short, there is a two-way interaction between precipitation and fire
332 activities on short timescales with different duration, forming a positive feedback loop.

333 We also conducted sensitivity simulations to investigate the underlying processes involved in the
334 fire-precipitation feedback. Fig. 7 shows the simulated difference in AOD (referred to as fire AOD)
335 between Case_Strong and Case_Weak. Both the spatial pattern and magnitude agree well with the
336 difference in AOD between strong and weak fire years based on CALIPSO observations.
337 Compared to the spatial patterns of fire consumption in Fig. 7, we can clearly see two transport
338 pathways of fire-emitted aerosols due to the continental divide by the Central Mexican Plateau.
339 North of 15°N, fire-emitted aerosols are transported northward by the subtropical high, among
340 which large amounts accumulate over the downstream Gulf of Mexico due to the block of the high
341 terrain, and the rest is further transported northward reaching the southeastern US; South of 15°N,
342 prevailing easterlies transport fire-emitted aerosols directly westward, far away to the eastern
343 Pacific.



344
345
346
347
348
349
350
351
352

Figure 7. Evaluation of model simulated fire-induced AOD. (a) Spatial distributions of differences in biomass burning AOD between strong and weak fire years from CALIPSO satellite data. (b) Differences in simulated AOD between Case_Strong and Case_Weak. Mean 850hPa wind vectors from (a) NCEP reanalysis data averaged in all years and (b) model simulations averaged between both cases are overlaid respectively. Stippling indicates the differences in AOD are statistically significant based on T-test.



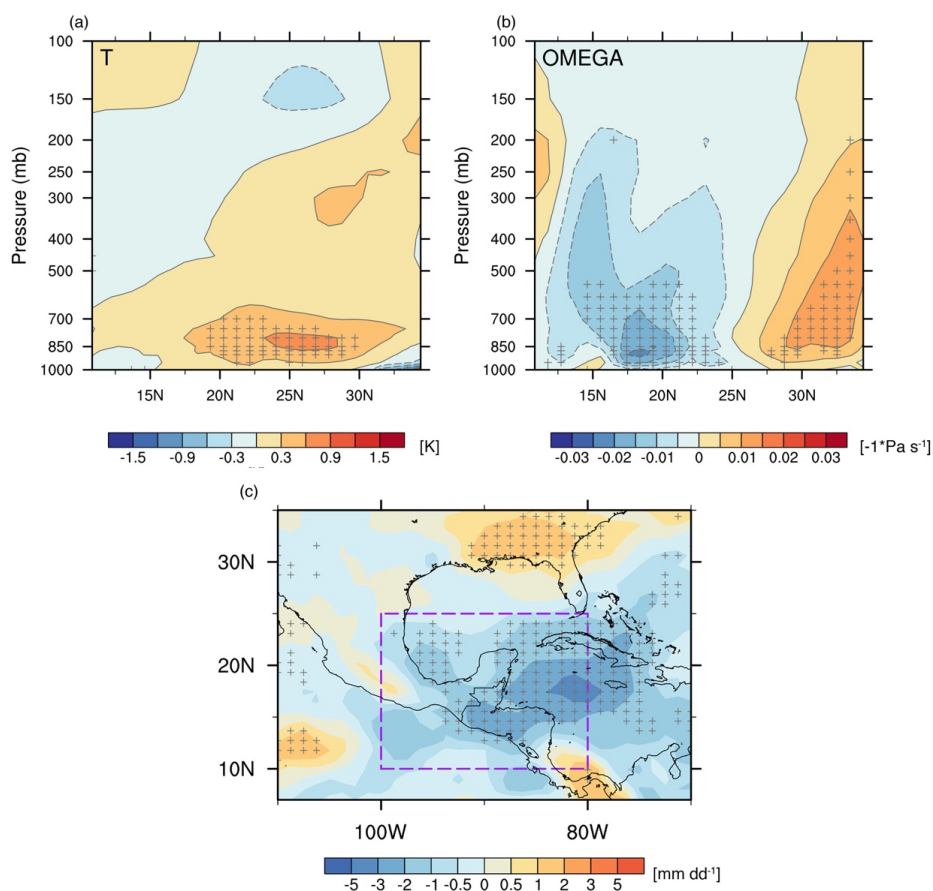
353
354
355
356
357
358
359

Figure 8. Changes in meteorological variables induced by fire-emitted aerosols. Differences in (a) atmospheric temperature and vertical pressure velocity (reversed signs and shaded colors) at different vertical levels between Case_Strong and Case_Weak. Changes in horizontal winds between the two cases are overlaid in (b). Stippling indicates the differences are statistically significant at the 90% confidence level based on T-test.



360

361 Considering the northward pathway, with the stack of light-absorbing BC aerosols, air temperature
362 warms up by approximately 1-2K, and this warming extends from 800hPa to 700hPa where BC
363 aerosols suspend (Fig. 8a-c). Vertical slices of the temperature anomalies indicate significant
364 warming to the north (downstream) of the fire source regions (Fig. 9a). In response to this warming,
365 the air above the fire aerosol layers rises up (Fig. 8d-f). The anomalous ascending motion covers
366 from the Gulf of Mexico to the southeastern US, with the maximum center located near the Gulf
367 of Mexico. This abnormal ascending motion, on one hand, enhances precipitation downstream of
368 the fire source regions, and on the other hand forces a compensating anomalous descending motion
369 over the SMCA region and suppresses the precipitation over the fire source regions (Fig. 9b-c).
370 This simulated opposite change in precipitation resembles the spatial pattern of the composited
371 precipitation difference between strong and weak fire years (Fig. 4a), suggesting that fire-
372 precipitation interaction reinforces the contrast of precipitation between strong and weak fire years.
373 Therefore, the model simulations confirm a positive fire-precipitation feedback loop on the short
374 timescale within the fire season.



375

376

377 **Figure 9.** Vertical slices of differences in (a) atmospheric temperature and (b) pressure velocity
 378 averaged along [80° -100° W] between Case_Strong and Case_Weak. (c) Differences in
 379 precipitation between Case_Strong and Case_Weak. Stippling indicates the differences are
 380 statistically significant based on T-test.

381

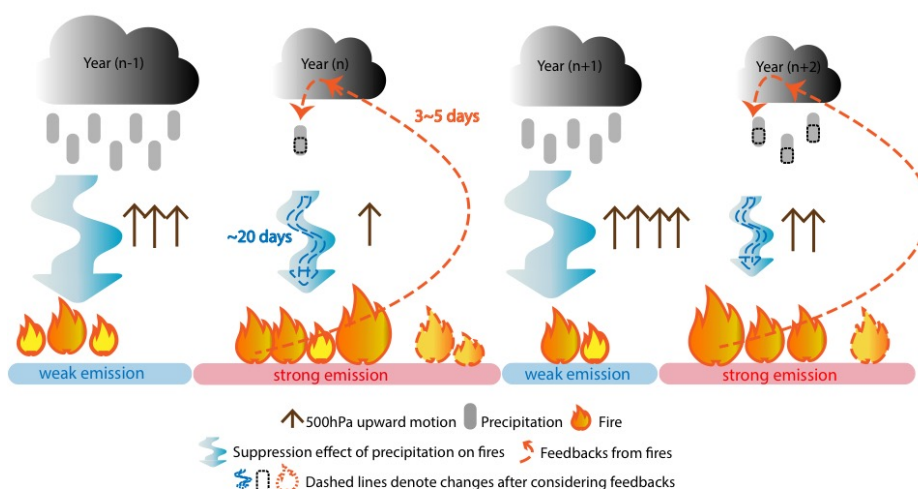
382 As illustrated in Fig. 10, originally on the interannual scale, fire activities over the SMCA region
 383 exhibit a significant quasi-biennial variability that is predominantly determined by the quasi-
 384 biennial variation of precipitation. On this basis, there is an additional two-way interaction between
 385 fire and precipitation on short timescales. Typically, precipitation suppresses fire activities with a
 386 time lag of more than 20 days, while fire-emitted aerosols suppress precipitation by modifying
 387 circulations with a timescale of 3-5 days. That is to say, for a year with abnormally weak
 388 precipitation, fire activities would get amplified, which in turn further weakens precipitation. In



389 this way, the short-term positive feedback loop ultimately enhances the quasi-biennial variability
 390 of precipitation and fire activities over the SMCA region.

391

392



393 **Figure 10.** A schematic diagram illustrating how multi-scale fire-precipitation interactions shape
 394 the quasi-biennial variability of fires over SMCA. On the interannual scale, the quasi-biennially
 395 varying precipitation triggers a similar quasi-biennially variability of fire activities via its
 396 suppression effect. Compared to adjacent years, a weaker precipitation year will facilitate stronger
 397 fires. On short timescales within each fire season, there is a positive feedback loop between fire
 398 and precipitation (denoted by dashed lines). The suppression effect of precipitation lasts long for
 399 approximately 20 days, while fires affect precipitation through a rapid adjustment of 3-5 days. In
 400 the weaker precipitation year, stronger fire activities emit more aerosols, which by mediating
 401 temperature and circulations, ultimately suppress precipitation over the fire source region. Such
 402 short-term interactions between precipitation and fire amplify the magnitude of anomalous fire and
 403 precipitation in individual years and enhance the quasi-biennial variability of both precipitation
 404 and fire.
 405



406 **4 Conclusion and Discussion**

407 Fires play an important role in the Earth system, and the complex interaction between fire activities
408 and ambient conditions poses a great challenge to fire prediction and management. This study
409 identifies a distinct quasi-biennial variability of fire activities over the SMCA region during 2003-
410 2019 on the basis of different fire metrics. Both the bottom-up (GFEDv4.1s) and top-down(QFED)
411 emission inventories show relatively higher fire consumption (or emission) in the odd-numbered
412 years than the adjacent even-numbered years with the only exception of the year 2016. Moreover,
413 fire-induced changes in AOD also reveal consistent quasi-biennial variation.

414 By examining the relationships between fire consumption and different meteorological variables,
415 our analysis indicates that the quasi-biennial signal is dominated by the quasi-biennially varying
416 precipitation, while the influence of temperature is mostly reflected in a few extremely strong fire
417 years. Typically, strong fire years correspond to suppressed upward motions and weakened
418 precipitation. The quasi-biennial variability of precipitation is seen in the time series of the regional
419 mean precipitation over SMCA and the spectral analysis, and is closely related to the EP-NP
420 teleconnection pattern in the two months previous to the fire season. The positive phase of the EP-
421 NP pattern implies enhanced precipitation over the southeastern US (downstream of the SMCA),
422 albeit reduced precipitation over the SMCA region.

423 On the other hand, we further found that positive feedback exists between fire-emitted aerosols
424 and precipitation on short timescales and acts to amplify the quasi-biennial oscillations in both fire
425 and precipitation over the SMCA region. Lead-lag correlations between daily fire emission and
426 precipitation suggest that the two-way interactions occur with different duration. The suppression
427 effect of precipitation lasts for approximately 20 days, while fire-emitted aerosols weaken
428 precipitation through rapid adjustments of 3-5 days. Furthermore, model simulations reveal that
429 compared to weak fire years, more fire-emitted aerosols are transported downstream and
430 accumulate near the Gulf of Mexico in strong fire years. These suspended light-absorbing BC
431 aerosols warm the low-level atmosphere by 1-2K and induce anomalous ascending motion aloft
432 700hPa. A compensating descending motion is subsequently forced over the SMCA region, which
433 ultimately suppresses the precipitation over the fire source region and hence forms a positive
434 feedback loop.



435 These findings provide useful information relevant to the fire control and mitigation of air quality
436 over the SMCA region. Given that fire activities over the SMCA represent a typical tropical fire
437 regime, our work may also provide new insight into some fundamental features of fires in the Earth
438 System. The mechanism may also operate elsewhere useful on the planet. While precipitation is
439 demonstrated to play the primary role in determining the periodicity of fire activities over the
440 SMCA region, the fundamental cause of the quasi-biennial variability of precipitation is unknown.
441 Currently, we have only shown that the EP-NP teleconnection, among all selected indexes, exerts
442 the most influence on the interannual variability of precipitation. Other teleconnection patterns,
443 e.g., ENSO, despite their insignificant correlations with SMCA precipitation, may affect the
444 circulation and precipitation over the southeastern US or over the neighboring Intra-American Sea
445 (Anthony Chen and Taylor, 2002), and hence might more or less affect the precipitation over the
446 SMCA region. Future efforts to quantify how different factors work together and shape the quasi-
447 biennial variability of precipitation would further benefit the prediction and management of fire
448 activities over the SMCA region.



449 **Data availability**

450 The GFED v4.1s fire emission data is available at <http://www.globalfiredata.org/data.html>.
451 The CRU TS v.4.06 can be found at <https://crudata.uea.ac.uk/cru/data/hrg/>. The QFEDv2.5 data
452 can be found at <http://ftp.as.harvard.edu/gcgrid/data/ExtData/HEMCO/QFED/v2018-07/>. The
453 AVHRR leaf area index is available from [https://www.ncei.noaa.gov/access/metadata/landing-
454 page/bin/iso?id=gov.noaa.ncdc:C01559](https://www.ncei.noaa.gov/access/metadata/landing-page/bin/iso?id=gov.noaa.ncdc:C01559). The MERRA-2 reanalysis data can be found at
455 https://gmao.gsfc.nasa.gov/reanalysis/MERRA-2/data_access/. The IMERG precipitation dataset
456 can be obtained from <https://gpm.nasa.gov/data/imerg>. The GPCP dataset can be obtained from
457 <https://www.ncei.noaa.gov/products/climate-data-records/precipitation-gpcp-daily>.
458 Teleconnection indices can be found at <https://psl.noaa.gov/data/climateindices/list/>. The NCEP-
459 NCAR reanalysis is obtained from
460 <https://www.esrl.noaa.gov/psd/data/gridded/data.ncep.reanalysis2.html>.
461 The CALIPSO product is available at
462 [https://asdc.larc.nasa.gov/project/CALIPSO/CAL_LID_L3_Tropospheric_APro_AllSky-
463 Standard-V4-20_V4-20](https://asdc.larc.nasa.gov/project/CALIPSO/CAL_LID_L3_Tropospheric_APro_AllSky-Standard-V4-20_V4-20).

464

465 **Author contribution**

466 Y.L. and Y. Q. conceived of the presented idea. Y. Q., Y. W. and Y. L. developed the theory. Y.
467 L. performed the computations and verified the methods. Y. Q., Y. L. and K. Z wrote the first draft
468 of the manuscript. All authors contributed to the interpretation of the results and writing/revision
469 of the final manuscript.

470

471 **Competing interests**

472 Yun Qian and Hailong Wang are members of the editorial board of Atmospheric Chemistry and
473 Physics. The authors have no other competing interests to declare.

474

475 **Acknowledgments**

476 We benefited from discussing some aspects of this work with John M Wallace and Dae-Hyun Kim.
477 This study is supported by the U.S. Department of Energy's Office of Science as part of the
478 Regional and Global Modeling and Analysis program. The Pacific Northwest National Laboratory
479 is operated for DOE by Battelle Memorial Institute under contract DE-AC05-76RL01830. We are
480 grateful to the High-Performance Computing (HPC) and the Massive Data Center (MDC) at
481 Nanjing University for doing the numerical calculations.

482

483

484

485



486 References

- 487 Abram, N. J., Henley, B. J., Sen Gupta, A., Lippmann, T. J. R., Clarke, H., Dowdy, A. J., Sharples, J. J., Nolan, R. H.,
488 Zhang, T. R., Wooster, M. J., Wurtzel, J. B., Meissner, K. J., Pitman, A. J., Ukkola, A. M., Murphy, B. P., Tapper, N.
489 J., and Boer, M. M.: Connections of climate change and variability to large and extreme forest fires in southeast
490 Australia, *Commun Earth Environ*, 2, ARTN 810.1038/s43247-020-00065-8, 2021.
- 491 Adler, R. F., Sapiano, M. R. P., Huffman, G. J., Wang, J. J., Gu, G. J., Bolvin, D., Chiu, L., Schneider, U., Becker,
492 A., Nelkin, E., Xie, P. P., Ferraro, R., and Shin, D. B.: The Global Precipitation Climatology Project (GPCP) Monthly
493 Analysis (New Version 2.3) and a Review of 2017 Global Precipitation, *Atmosphere*, 9, ARTN
494 13810.3390/atmos9040138, 2018.
- 495 Adler, R. W., Jian-Jian; Sapiano, Mathew; Huffman, George; Bolvin, David; Nelkin, Eric; and NOAA CDR Program:
496 Global Precipitation Climatology Project (GPCP) Climate Data Record (CDR), Version 1.3 (Daily), NOAA National
497 Centers for Environmental Information. doi:10.7289/V5RX998Z, 2017.
- 498 Aguilera, R., Corringham, T., Gershunov, A., and Benmarhnia, T.: Wildfire smoke impacts respiratory health more
499 than fine particles from other sources: observational evidence from Southern California, *Nature Communications*, 12,
500 ARTN 149310.1038/s41467-021-21708-0, 2021.
- 501 Amador, J. A., Alfaro, E. J., Lizano, O. G., and Magana, V. O.: Atmospheric forcing of the eastern tropical Pacific: A
502 review, *Prog Oceanogr*, 69, 101-142, 10.1016/j.pocean.2006.03.007, 2006.
- 503 Anthony Chen, A. and Taylor, M. A.: Investigating the link between early season Caribbean rainfall and the El Niño
504 + 1 year, *International Journal of Climatology*, 22, 87-106, 10.1002/joc.711, 2002.
- 505 Archibald, S.: Managing the human component of fire regimes: lessons from Africa, *Philosophical Transactions of
506 the Royal Society B: Biological Sciences*, 371, 20150346, 2016.
- 507 Athanasiadis, P. J., Wallace, J. M., and Wettstein, J. J.: Patterns of Wintertime Jet Stream Variability and Their
508 Relation to the Storm Tracks, *J Atmos Sci*, 67, 1361-1381, 10.1175/2009jas3270.1, 2010.
- 509 Bond, T. C., Doherty, S. J., Fahey, D., Forster, P., Berntsen, T., DeAngelo, B., Flanner, M., Ghan, S., Kärcher, B.,
510 and Koch, D.: Bounding the role of black carbon in the climate system: A scientific assessment, *Journal of Geophysical
511 Research: Atmospheres*, 118, 5380-5552, 2013.
- 512 Bowman, D. M., Balch, J. K., Artaxo, P., Bond, W. J., Carlson, J. M., Cochrane, M. A., D'Antonio, C. M., DeFries,
513 R. S., Doyle, J. C., and Harrison, S. P.: Fire in the Earth system, *science*, 324, 481-484, 2009.
- 514 Bowman, D. M. J. S., Williamson, G. J., Abatzoglou, J. T., Kolden, C. A., Cochrane, M. A., and Smith, A. M. S.:
515 Human exposure and sensitivity to globally extreme wildfire events, *Nat Ecol Evol*, 1, ARTN 005810.1038/s41559-
516 016-0058, 2017.
- 517 Cary, G. J., Keane, R. E., Gardner, R. H., Lavorel, S., Flannigan, M. D., Davies, I. D., Li, C., Lenihan, J. M., Rupp,
518 T. S., and Mouillot, F.: Comparison of the sensitivity of landscape-fire-succession models to variation in terrain, fuel
519 pattern, climate and weather, *Landscape ecology*, 21, 121-137, 2006.
- 520 Crouse, J., DeCarlo, P., Blake, D. R., Emmons, L., Campos, T., Apel, E., Clarke, A., Weinheimer, A., McCabe, D.,
521 and Yokelson, R. J.: Biomass burning and urban air pollution over the Central Mexican Plateau, *Atmospheric
522 Chemistry and Physics*, 9, 4929-4944, 2009.
- 523 Crutzen, P. J. and Andreae, M. O.: Biomass Burning in the Tropics - Impact on Atmospheric Chemistry and
524 Biogeochemical Cycles, *Science*, 250, 1669-1678, DOI 10.1126/science.250.4988.1669, 1990.
- 525 Danabasoglu, G., Lamarque, J. F., Bacmeister, J., Bailey, D. A., DuVivier, A. K., Edwards, J., Emmons, L. K., Fasullo,
526 J., Garcia, R., Gettelman, A., Hannay, C., Holland, M. M., Large, W. G., Lauritzen, P. H., Lawrence, D. M., Lenaerts,
527 J. T. M., Lindsay, K., Lipscomb, W. H., Mills, M. J., Neale, R., Oleson, K. W., Otto-Bliesner, B., Phillips, A. S.,
528 Sacks, W., Tilmes, S., van Kampenhou, L., Vertenstein, M., Bertini, A., Dennis, J., Deser, C., Fischer, C., Fox-
529 Kemper, B., Kay, J. E., Kinnison, D., Kushner, P. J., Larson, V. E., Long, M. C., Mickelson, S., Moore, J. K.,
530 Nienhouse, E., Polvani, L., Rasch, P. J., and Strand, W. G.: The Community Earth System Model Version 2 (CESM2),
531 *J Adv Model Earth Sy*, 12, ARTN e2019MS00191610.1029/2019MS001916, 2020.



- 532 Ding, K., Huang, X., Ding, A. J., Wang, M. H., Su, H., Kerminen, V. M., Petaja, T., Tan, Z. M., Wang, Z. L., Zhou,
533 D. R., Sun, J. N., Liao, H., Wang, H. J., Carslaw, K., Wood, R., Zuidema, P., Rosenfeld, D., Kulmala, M., Fu, C. B.,
534 Poschl, U., Cheng, Y. F., and Andreae, M. O.: Aerosol-boundary-layer-monsoon interactions amplify semi-direct
535 effect of biomass smoke on low cloud formation in Southeast Asia, *Nature Communications*, 12, ARTN
536 641610.1038/s41467-021-26728-4, 2021.
- 537 Duran-Quesada, A. M., Gimeno, L., and Amador, J.: Role of moisture transport for Central American precipitation,
538 *Earth Syst Dynam*, 8, 147-161, 10.5194/esd-8-147-2017, 2017.
- 539 Fang, K. Y., Yao, Q. C., Guo, Z. T., Zheng, B., Du, J. H., Qi, F. Z., Yan, P., Li, J., Ou, T. H., Liu, J., He, M. S., and
540 Trouet, V.: ENSO modulates wildfire activity in China, *Nature Communications*, 12, ARTN 176410.1038/s41467-
541 021-21988-6, 2021.
- 542 Fasullo, J. T., Rosenbloom, N., and Buchholz, R.: A multiyear tropical Pacific cooling response to recent Australian
543 wildfires in CESM2, *Science Advances*, 9, eadg1213, 2023.
- 544 Flannigan, M. D., Krawchuk, M. A., de Groot, W. J., Wotton, B. M., and Gowman, L. M.: Implications of changing
545 climate for global wildland fire, *International journal of wildland fire*, 18, 483-507, 2009.
- 546 Flannigan, M. D., Logan, K. A., Amiro, B. D., Skinner, W. R., and Stocks, B.: Future area burned in Canada, *Climatic*
547 *change*, 72, 1-16, 2005.
- 548 Gelaro, R., McCarty, W., Suarez, M. J., Todling, R., Molod, A., Takacs, L., Randles, C. A., Darmenov, A., Bosilovich,
549 M. G., Reichle, R., Wargan, K., Coy, L., Cullather, R., Draper, C., Akella, S., Buchard, V., Conaty, A., da Silva, A.
550 M., Gu, W., Kim, G. K., Koster, R., Lucchesi, R., Merkova, D., Nielsen, J. E., Partyka, G., Pawson, S., Putman, W.,
551 Rienecker, M., Schubert, S. D., Sienkiewicz, M., and Zhao, B.: The Modern-Era Retrospective Analysis for Research
552 and Applications, Version 2 (MERRA-2), *J Climate*, 30, 5419-5454, 10.1175/Jcli-D-16-0758.1, 2017.
- 553 Giglio, L., Randerson, J. T., and Werf, G. R.: Analysis of daily, monthly, and annual burned area using the fourth -
554 generation global fire emissions database (GFED4), *Journal of Geophysical Research: Biogeosciences*, 118, 317-328,
555 2013.
- 556 Gillett, N., Weaver, A., Zwiers, F., and Flannigan, M.: Detecting the effect of climate change on Canadian forest fires,
557 *Geophysical Research Letters*, 31, 2004.
- 558 Harris, I., Jones, P., Osborn, T., and Lister, D.: Updated high - resolution grids of monthly climatic observations -
559 the CRU TS3. 10 Dataset, *International Journal of Climatology*, 34, 623-642, 2014.
- 560 Hersbach, H., Bell, B., Berrisford, P., Hirahara, S., Horanyi, A., Muñoz-Sabater, J., Nicolas, J., Peubey, C., Radu, R.,
561 Schepers, D., Simmons, A., Soci, C., Abdalla, S., Abellan, X., Balsamo, G., Bechtold, P., Biavati, G., Bidlot, J.,
562 Bonavita, M., De Chiara, G., Dahlgren, P., Dee, D., Diamantakis, M., Dragani, R., Flemming, J., Forbes, R., Fuentes,
563 M., Geer, A., Haimberger, L., Healy, S., Hogan, R. J., Holm, E., Janiskova, M., Keeley, S., Laloyaux, P., Lopez, P.,
564 Lupu, C., Radnoti, G., de Rosnay, P., Rozum, I., Vamborg, F., Villaume, S., and Thepaut, J. N.: The ERA5 global
565 reanalysis, *Quarterly Journal of the Royal Meteorological Society*, 146, 1999-2049, 10.1002/qj.3803, 2020.
- 566 Huang, X., Ding, K., Liu, J. Y., Wang, Z. L., Tang, R., Xue, L., Wang, H. K., Zhang, Q., Tan, Z. M., Fu, C. B., Davis,
567 S. J., Andreae, M. O., and Ding, A. J.: Smoke-weather interaction affects extreme wildfires in diverse coastal regions,
568 *Science*, 379, 457-461, 10.1126/science.add9843, 2023.
- 569 Huffman, G. J., Bolvin, D. T., Nelkin, E. J., and Tan, J.: Integrated Multi-satellite Retrievals for GPM (IMERG)
570 technical documentation, *Nasa/Gsfc Code*, 612, 2019, 2015.
- 571 Huffman, G. J., Bolvin, D. T., Braithwaite, D., Hsu, K.-L., Joyce, R. J., Kidd, C., Nelkin, E. J., Sorooshian, S., Stocker,
572 E. F., and Tan, J.: Integrated multi-satellite retrievals for the global precipitation measurement (GPM) mission
573 (IMERG), *Satellite Precipitation Measurement: Volume 1*, 343-353, 2020.
- 574 Ichoku, C., Ellison, L. T., Willmot, K. E., Matsui, T., Dezfuli, A. K., Gatebe, C. K., Wang, J., Wilcox, E. M., Lee, J.,
575 and Adegoke, J.: Biomass burning, land-cover change, and the hydrological cycle in Northern sub-Saharan Africa,
576 *Environmental Research Letters*, 11, 095005, 2016.
- 577 Jiang, Y. Q., Yang, X. Q., Liu, X. H., Qian, Y., Zhang, K., Wang, M. H., Li, F., Wang, Y., and Lu, Z.: Impacts of
578 Wildfire Aerosols on Global Energy Budget and Climate: The Role of Climate Feedbacks, *J Climate*, 33, 3351-3366,
579 10.1175/Jcli-D-19-0572.1, 2020.



- 580 Jolly, W. M., Cochrane, M. A., Freeborn, P. H., Holden, Z. A., Brown, T. J., Williamson, G. J., and Bowman, D. M.
581 J. S.: Climate-induced variations in global wildfire danger from 1979 to 2013, *Nature Communications*, 6, ARTN
582 753710.1038/ncomms8537, 2015.
- 583 Kanamitsu, M., Ebisuzaki, W., Woollen, J., Yang, S.-K., Hnilo, J., Fiorino, M., and Potter, G.: NCEP–DOE AMIP-II
584 Reanalysis (R-2), *B Am Meteorol Soc*, 83, 1631-1644, 2002.
- 585 Knorr, W., Dentener, F., Lamarque, J. F., Jiang, L. W., and Arneth, A.: Wildfire air pollution hazard during the 21st
586 century, *Atmos Chem Phys*, 17, 9223-9236, 10.5194/acp-17-9223-2017, 2017.
- 587 Koster, R. D., Darnenov, A. S., and da Silva, A. M.: The quick fire emissions dataset (QFED): Documentation of
588 versions 2.1, 2.2 and 2.4, 2015.
- 589 Kreidenweis, S. M., Remer, L. A., Bruintjes, R., and Dubovik, O.: Smoke aerosol from biomass burning in Mexico:
590 Hygroscopic smoke optical model, *Journal of Geophysical Research: Atmospheres*, 106, 4831-4844, 2001.
- 591 Lee, Y. S., Collins, D. R., Li, R., Bowman, K. P., and Feingold, G.: Expected impact of an aged biomass burning
592 aerosol on cloud condensation nuclei and cloud droplet concentrations, *Journal of Geophysical Research:*
593 *Atmospheres*, 111, 2006.
- 594 Liu, Y. W., Zhang, K., Qian, Y., Wang, Y. H., Zou, Y. F., Song, Y. J., Wan, H., Liu, X. H., and Yang, X. Q.:
595 Investigation of short-term effective radiative forcing of fire aerosols over North America using nudged hindcast
596 ensembles, *Atmos Chem Phys*, 18, 31-47, 10.5194/acp-18-31-2018, 2018.
- 597 Lu, Z., Liu, X., Zhang, Z., Zhao, C., Meyer, K., Rajapakshe, C., Wu, C., Yang, Z., and Penner, J. E.: Biomass smoke
598 from southern Africa can significantly enhance the brightness of stratocumulus over the southeastern Atlantic Ocean,
599 *Proceedings of the National Academy of Science*, 201713703, 2018.
- 600 Magi, B., Rabin, S., Shevliakova, E., and Pacala, S.: Separating agricultural and non-agricultural fire seasonality at
601 regional scales, *Biogeosciences*, 9, 3003, 2012.
- 602 Marlon, J. R., Bartlein, P. J., Carcaillet, C., Gavin, D. G., Harrison, S. P., Higuera, P. E., Joos, F., Power, M., and
603 Prentice, I.: Climate and human influences on global biomass burning over the past two millennia, *Nature Geoscience*,
604 1, 697-702, 2008.
- 605 Mouillot, F. and Field, C. B.: Fire history and the global carbon budget: a 1×1 fire history reconstruction for the 20th
606 century, *Global Change Biology*, 11, 398-420, 2005.
- 607 Page, S. E., Siegert, F., Rieley, J. O., Boehm, H. D. V., Jaya, A., and Limin, S.: The amount of carbon released from
608 peat and forest fires in Indonesia during 1997, *Nature*, 420, 61-65, 10.1038/nature01131, 2002.
- 609 Pechony, O. and Shindell, D.: Fire parameterization on a global scale, *Journal of Geophysical Research: Atmospheres*,
610 114, 2009.
- 611 Perdigon-Morales, J., Romero-Centeno, R., Barrett, B. S., and Ordonez, P.: Intraseasonal Variability of Summer
612 Precipitation in Mexico: MJO Influence on the Midsummer Drought, *J Climate*, 32, 2313-2327, 10.1175/Jcli-D-18-
613 0425.1, 2019.
- 614 Power, M. J., Marlon, J., Ortiz, N., Bartlein, P. J., Harrison, S. P., Mayle, F. E., Ballouche, A., Bradshaw, R. H.,
615 Carcaillet, C., and Cordova, C.: Changes in fire regimes since the Last Glacial Maximum: an assessment based on a
616 global synthesis and analysis of charcoal data, *Climate dynamics*, 30, 887-907, 2008.
- 617 Prasad, V. K., Badarinath, K., and Eaturu, A.: Biophysical and anthropogenic controls of forest fires in the Deccan
618 Plateau, India, *Journal of Environmental Management*, 86, 1-13, 2008.
- 619 Randerson, J., Chen, Y., Werf, G., Rogers, B., and Morton, D.: Global burned area and biomass burning emissions
620 from small fires, *Journal of Geophysical Research: Biogeosciences*, 117, 2012.
- 621 Rogers, C. M. and Bowman, K. P.: Transport of smoke from the Central American fires of 1998, *Journal of*
622 *Geophysical Research: Atmospheres*, 106, 28357-28368, 2001.
- 623 Tosca, M., Randerson, J., Zender, C., Flanner, M., and Rasch, P. J.: Do biomass burning aerosols intensify drought in
624 equatorial Asia during El Nino?, *Atmospheric Chemistry and Physics*, 10, 3515-3528, 2010.



- 625 Tosca, M. G., Randerson, J. T., and Zender, C. S.: Global impact of smoke aerosols from landscape fires on climate
626 and the Hadley circulation, *Atmos Chem Phys*, 13, 5227-5241, 10.5194/acp-13-5227-2013, 2013.
- 627 van Marle, M. J. E., Kloster, S., Magi, B. I., Marlon, J. R., Daniau, A. L., Field, R. D., Armeth, A., Forrest, M., Hantson,
628 S., Kehrwald, N. M., Knorr, W., Lasslop, G., Li, F., Mangeon, S., Yue, C., Kaiser, J. W., and van der Werf, G. R.:
629 Historic global biomass burning emissions for CMIP6 (BB4CMIP) based on merging satellite observations with
630 proxies and fire models (1750-2015), *Geosci Model Dev*, 10, 3329-3357, 10.5194/gmd-10-3329-2017, 2017.
- 631 Veira, A., Lasslop, G., and Kloster, S.: Wildfires in a warmer climate: Emission fluxes, emission heights, and black
632 carbon concentrations in 2090–2099, *Journal of Geophysical Research: Atmospheres*, 121, 3195-3223, 2016.
- 633 Vermote, E.: NOAA CDR Program: NOAA Climate Data Record (CDR) of AVHRR Leaf Area Index (LAI) and
634 Fraction of Absorbed Photosynthetically Active Radiation (FAPAR), Version 5, Version, 5, NOAA National Centers
635 for Environmental Information. , 2019.
- 636 Voulgarakis, A. and Field, R. D.: Fire influences on atmospheric composition, air quality and climate, *Current
637 Pollution Reports*, 1, 70-81, 2015.
- 638 Winker, D. M., Tackett, J. L., Getzewich, B. J., Liu, Z., Vaughan, M. A., and Rogers, R. R.: The global 3-D distribution
639 of tropospheric aerosols as characterized by CALIOP, *Atmos Chem Phys*, 13, 3345-3361, 10.5194/acp-13-3345-2013,
640 2013.
- 641 Yokelson, R., Urbanski, S., Atlas, E., Toohey, D., Alvarado, E., Crounse, J., Wennberg, P., Fisher, M., Wold, C., and
642 Campos, T.: Emissions from forest fires near Mexico City, *Atmos. Chem. Phys*, 7, 5569-5584, 2007.
- 643 Yokelson, R. J., Crounse, J., DeCarlo, P., Karl, T., Urbanski, S., Atlas, E., Campos, T., Shinozuka, Y., Kasputin, V.,
644 and Clarke, A.: Emissions from biomass burning in the Yucatan, *Atmospheric Chemistry and Physics*, 9, 5785, 2009.
- 645 Yue, S., Zhu, J., Chen, S., Xie, Q., Li, W., Li, L., Ren, H., Su, S., Li, P., and Ma, H.: Brown carbon from biomass
646 burning imposes strong circum-Arctic warming, *One Earth*, 5, 293-304, 2022.
- 647 Zhang, Y. W., Fan, J. W., Shrivastava, M., Homeyer, C. R., Wang, Y., and Seinfeld, J. H.: Notable impact of wildfires
648 in the western United States on weather hazards in the central United States, *P Natl Acad Sci USA*, 119, ARTN
649 e220732911910.1073/pnas.2207329119, 2022.
- 650 Zhong, Q. R., Schutgens, N., van der Werf, G., van Noije, T., Tsigaridis, K., Bauer, S. E., Mielonen, T., Kirkevag, A.,
651 Seland, O., Kokkola, H., Checa-Garcia, R., Neubauer, D., Kipling, Z., Matsui, H., Ginoux, P., Takemura, T., Le Sager,
652 P., Remy, S., Bian, H. S., Chin, M., Zhang, K., Zhu, J. L., Tsyro, S. G., Curci, G., Protonotariou, A., Johnson, B.,
653 Penner, J. E., Bellouin, N., Skeie, R. B., and Myhre, G.: Satellite-based evaluation of AeroCom model bias in biomass
654 burning regions, *Atmos Chem Phys*, 22, 11009-11032, 10.5194/acp-22-11009-2022, 2022.
- 655